Markvart, Aleksandr; Song, Mingzhao; Glybovski, Stanislav; Belov, Pavel; Simovski, Constantin; Kapitanova, Polina

Metasurface for Near-Field Wireless Power Transfer with Reduced Electric Field Leakage

Published in:
IEEE Access

DOI:
10.1109/ACCESS.2020.2976755

Published: 01/01/2020

Document Version
Publisher's PDF, also known as Version of record

IEEE Access
Multidisciplinary : Rapid Review : Open Access Journal

Received February 2, 2020, accepted February 20, 2020, date of publication February 27, 2020, date of current version March 6, 2020.

Digital Object Identifier 10.1109/ACCESS.2020.2976755

Metasurface for Near-Field Wireless Power Transfer With Reduced Electric Field Leakage

ALEKSANDR MARKVART[1], MINGZHAO SONG[1], STANISLAV GLYBOVSKI[1], PAVEL BELOV[1], CONSTANTIN SIMOVSKI[1,2], AND POLINA KAPITANOVA[1]

[1]Faculty of Physics and Engineering, ITMO University, 197101 St. Petersburg, Russia
[2]Research Center of Electronics and Nanoengineering, School of Electrical Engineering, Aalto University, 00076 Aalto, Finland

Corresponding authors: Mingzhao Song (m.song@metalab.ifmo.ru) and Polina Kapitanova (p.kapitanova@metalab.ifmo.ru)

This work was supported by the Russian Science Foundation under Project 17-79-20379.

ABSTRACT Wireless power transfer is a breakthrough technology which can be used in all aspects of humans daily life. Here, a bi-layer metasurface as a transmitter for near-field wireless power transfer is proposed and studied. The novelty and advantage of the proposed metasurface is the spatial separation of the electric and magnetic near fields. Magnetic fields responsible for power transfer are sufficiently high on top of the metasurface whereas the electric fields are almost completely confined between two layers of the metasurface. These unique properties have been obtained due to the special metasurface design based on two orthogonal layers of resonant wires immersed in high-permittivity background. The theoretical and experimental study reveal the quasi-uniform magnetic field distribution over the metasurface dimensions of 40×40 cm^2 that makes it suitable for wireless power transfer via resonant magnetic coupling to one or several receivers placed above it. Compared with a conventional planar spiral coil solution, the specific absorption rate of the proposed metasurface is reduced by 47 times, which enables to greatly increase the allowable transferred power without violating the safety regulation and reducing the efficiency.

INDEX TERMS Metasurface, electromagnetic safety, wireless power transfer.

I. INTRODUCTION

Crrently, a great variety of portable electronic devices are of daily use. Wireless power transfer (WPT) technology could be the solution for remote charging several devices at once [1]–[4]. WPT charging pads available in stock normally charge one device over the distance within a few millimetres by means of inductive coupling between transmitting and receiving coils. To increase the charging distance up to several centimetres, various approaches based on different physics have been proposed, e.g. magnetic resonant coupling mechanism [5], [6], metamaterials applied as a field enhancer [7]–[10], and the use of nonlinear parity-time-symmetric circuits [11], [12]. If multiple devices need to be charged simultaneously on the same pad, the transmitting (Tx) coil must be large enough to accommodate them. This poses a challenge as to uniform power delivery to devices regardless of their positions. The electromagnetic field distribution in the plane parallel to the pad must be as uniform as possible. This idea has been implemented by large spiral multi-turn coils of different geometries [13]–[19]. However, the resonant magnetic field provided by large coils is spatially accompanied by a resonant electric field in the same area, which leads to an increased field-induced heat in adjacent human tissues [20]. Another important issue is maximal allowable transferred power under safety regulation. It has been demonstrated that safety concern is one of the major factors that limits the input power [20]–[25]. Thus, minimizing the electromagnetic exposure of human tissues is of great importance for increasing the allowable transferred power of on-desk charging systems.

In this paper, a metasurface is designed as a transmitter or a charging station which allows a much higher input power under the same safety regulation. To support charging multiple receivers, a quasi-uniform magnetic field can be generated and distributed on the surface (see Fig. 1),

The associate editor coordinating the review of this manuscript and approving it for publication was Lin Peng.

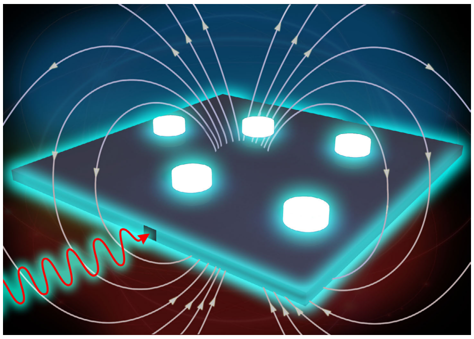

FIGURE 1. Conceptual photograph of a metasurface smart table simultaneously powering multiple free-positioned devices.

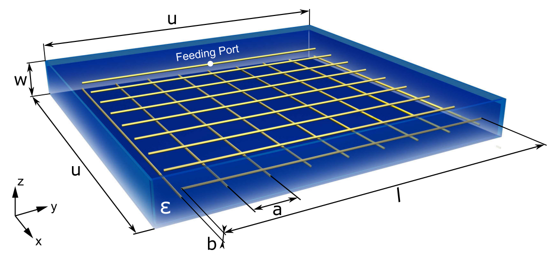

FIGURE 2. Design of the metasurface.

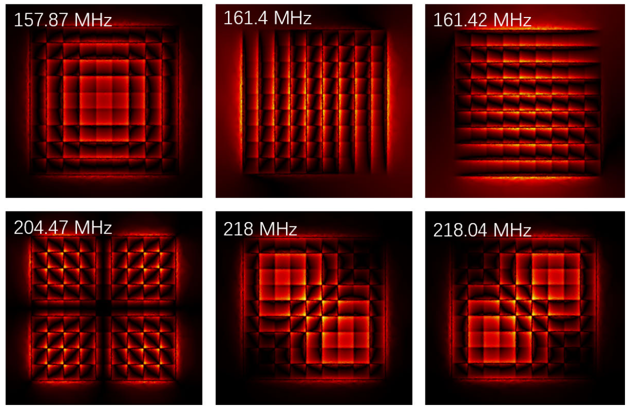

FIGURE 3. Simulated z-component of magnetic field for the first six modes of the metasurface. The plotted distributions are in the middle plane between the wire arrays.

which allows a steady WPT efficiency from transmitter to the receiver regardless of their positions in the plane parallel to the metasurface. The novelty of the proposed metasurface is a strong separation of the electric and magnetic near fields: the former can be mostly confined within the metasurface. It helps to dramatically improve safety issues. The numerical and experimental studies of the metasurface modes, electromagnetic field distributions, as well as WPT efficiency from metasurface to a receiver are performed. The safety level of the proposed structure is also evaluated in terms of specific absorption rate (SAR) and electric field distributions compared with a conventional spiral transmitting coil.

II. DESIGN AND ANALYSIS OF METASURFACE

Recently, bulky wire media have been intensively studied for different purposes, from sub-wavelength imaging [26] to enhanced Purcell effect [27]. We propose a metasurface based on bi-layer resonant wire arrays. For a single layer of wires, due to the placement of identical wires on a scale much smaller than the wavelength, a giant coupling between each resonant wires occurs. Therefore, the original resonant frequency of a single wire splits into different bands which corresponds to different eigenmodes. For all these modes, the magnetic fields are always concentrated in the center, whereas the electric field is located at the end of the wires [28]. To further shield the electric field and change the mode profile, we propose to use bi-layer structure of wire arrays, so that the electric field can be confined not only at edges of the wires, but also constrained between two layers. As shown in Fig. 2, the top layer is orthogonally placed on and electrically couples to the bottom one. The electric current of the eigenmode of each layer provides an equivalent inductance, and the coupling between two layers provides an equivalent capacitance. Therefore, the overall resonant frequency of the structure can be defined by choosing the mode and their coupling distance. Both layers are immersed in the host medium with permittivity of ε for a broader resonant frequency range control. Each layer consists of 10 equally distributed copper wires with a radius of $r = 1$ mm, a length of $l = 50$ cm and period $a = 5.56$ cm. The spacing between two layers in the direction normal to the their planes is $b = 8$ mm. The overall area of the metasurface is 50×50 cm^2, which is sufficient for transferring power to several receivers of the size of smartphones. In a conventional spiral coil, the electric and magnetic fields are both enhanced at the resonance frequency in the same spatial area. In the proposed metasurface, besides a quasi-uniform (where the field intensity drops to half of its maximal value) magnetic field in a large area, the sandwiched structure of the metasurface grants an effective capacitance in all overlapping parts between the top and bottom layers, in which the electric field is confined. By properly choosing the resonant modes, a quasi-uniform magnetic field distribution can be obtained.

We first numerically studied the normal modes of the metasurface with air as a host medium for the wires using Eigenmode Solver in CST Microwave Studio 2017. Since these parallel wires are closely placed on a scale much smaller than the wavelength, a giant coupling between all the wires occurs. Therefore, the original resonance frequency splits into several bands, which corresponds to the different eigenmodes as shown in Fig. 3. The fundamental mode of the metasurface was found resonating at 157 MHz. At this frequency the currents were excited in both arrays of wires simultaneously. Due to the strong coupling between the wire arrays, the currents flowing on the top layer together with that on the bottom layer formed five equivalent in-phase current frames, as shown in Fig.4(a). The co-directional current flowing around the frames created mainly a vertical magnetic field, which is quasi-uniform in the plane above the metasurface.

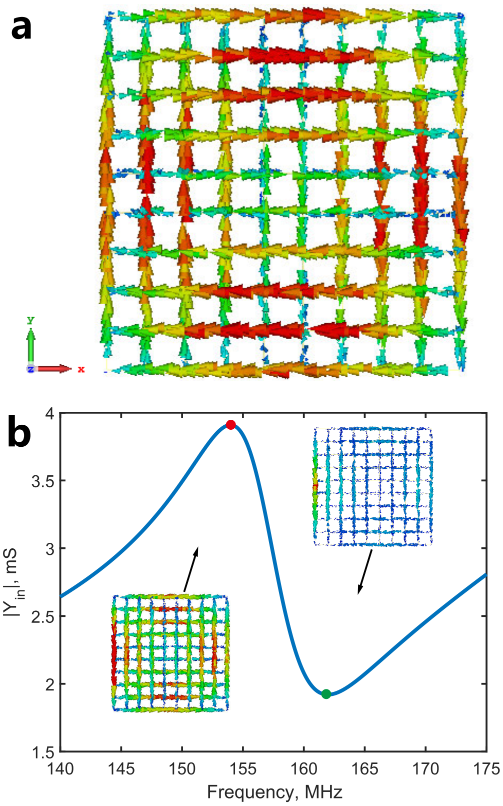

FIGURE 4. (a) Surface current distribution on the fundamental mode at 155 MHz. (b) Simulated input admittance of the metasurface excited by a lateral current wire. The insets show the current distributions at series and parallel resonances corresponding to 154 MHz and 162 MHz, respectively.

To excite this mode, a 50 Ohm port was inserted in the middle point of a lateral wire which drives an alternating current on this wire. The characteristics of the metasurface, such as the resonant frequency, electric and magnetic field distributions were numerically calculated in Frequency Domain Solver of CST Microwave Studio.

From the calculated input admittance as shown in Fig. 4(b), two peaks can be found around the frequency of 155 MHz, which results from the hybridization between the mode of the other 19 wires and the feeding wire of the same layer with the port. Maximum and minimum in the input admittance spectrum correspond to series and parallel resonances, respectively. In Fig. 4(b), the insets show the wire current distributions at two resonances. It can be seen that at the series resonance, the current of the feeding wires and of the other wires are in phase that contributes a higher and more homogeneous magnetic field than the parallel resonance. Thus, the series resonance is chosen for further investigation.

Next, we proceed to investigate the influence of the permittivity of the host medium. When the host medium is air, the wire length is comparable to half-wavelength in free space resulting in a high radiation loss even in the presence of a matched inductively-coupled receiving loop over the metasurface.

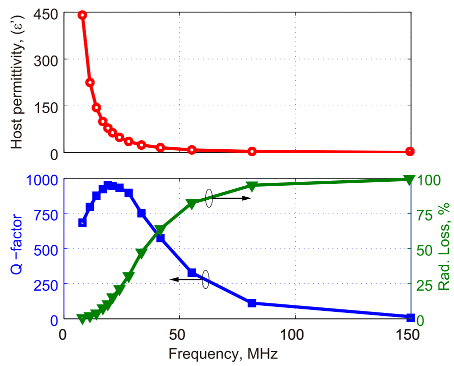

FIGURE 5. Simulated dependence of host permittivity ε', Q-factor and radiation loss at the resonant frequency.

Moreover, the resonant frequency of 155 MHz is far away from the existing standards or regulations (205 kHz for Qi standard, 6.78 MHz for A4WP standard, 19 MHz for Russian) and has to be shifted down.

To minimize the radiation loss and decrease resonant frequency, the electric size of the metasurface should be reduced. For this purpose, the wire arrays were immersed into a dielectric host with high permittivity. The corresponding resonant frequency, Q-factor and radiation efficiency as functions of the host permittivity were numerically investigated and are shown in Fig.5. The lossless dielectric host medium was considered and its permittivity ranged from 1 to 450. The resonant frequency of the metasurface was determined at the maximum of the input admittance spectrum. The Q-factor was extracted from the input admittance [29]. The radiation loss was calculated directly in CST Microwave Studio.

At resonant frequency, Q-factor can be represented by:

$$Q = \frac{\omega(\varepsilon)L}{R_r(\varepsilon) + R_o} \tag{1}$$

where R_o denotes ohmic loss and R_r radiation loss. If the equivalent inductance L, ohmic loss, and radiation loss remain unchanged, the Q-factor is linearly proportional to the resonant frequency ω. Thus, as the permittivity decreases, the resonant frequency increases correspondingly, which explains the increasing tendency in the beginning stage of the blue curve in Fig. 5. However, the decreasing tendency results from two factors. First, the electrical size of the wires increases as the permittivity decreases leading to a significant radiation loss, as shown in the green curve in Fig. 5. Second, as the resonant frequency increases, the skin depth effect increases correspondingly leading to an increased equivalent resistance. Therefore, there exists a maximal Q-factor corresponding to an optimal permittivity. For the given dimensions of the metasurface, the maximal Q-factor is achieved at the frequency of 20 MHz for the permittivity $\varepsilon = 80$ with no loss.

In this study we consider water as a host material. It is known that at megahertz frequencies it is characterised by relatively high permittivity and low loss. However, exact water properties depend on many factors: temperature, purity, air pressure, and operational frequency [30]. For example,

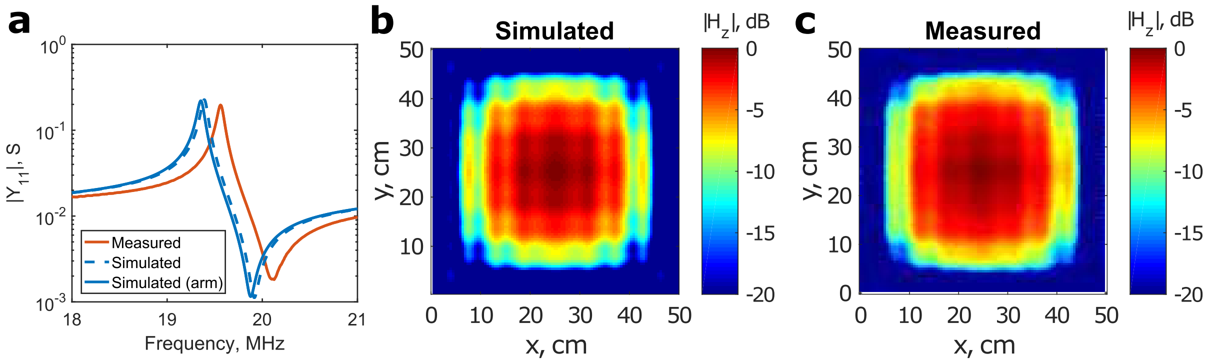

FIGURE 6. **(a) Simulated and measured input admittance of the metasurface. Simulated (b) and measured (c) distributions of the z-component of normalized magnetic fields.**

at room temperature, de-ionized water has relative dielectric constant $\varepsilon = 80.1 + j0.03$ at 27MHz. Fresh tap water under the same conditions is characterised by relative dielectric constant $\varepsilon = 79.6 + j18.9$ [31]. Apparently, the loss factor of water will influence the Q-factor. The water permittivity measurement was conducted with SPEAG Dielectric Assessment Kit connected to Agilent E8362C Vector Network Analyser (VNA). The de-ionized water sample was measured in the frequency range 10-200 MHz under the room temperature. At the frequency 20 MHz the measured water permittivity was $\varepsilon = 79.6 + j0.22$. We used this value for the numerical study of the metasurface performance based on the wire arrays immersed in the center of the water layer with the dimensions of 60 cm × 60 cm × 2.4 cm. Fig. 6 (a) shows the simulated input admittance of the metasurface fed by a lumped port in a lateral wire gap. The first peak frequency of 19.2 MHz is specified as the WPT operational frequency. The calculated Q-factor taking into account the water losses is 282. The discrepancy to the influence of the host losses, it is still high enough and stays at the level of Tx coil implementations such as spiral coils [32], [33]. The simulated magnetic field distribution at the resonant frequency normalized to its maximum at the center is presented in Fig. 6 (b). In the central working area on the metasurface, the magnetic field has quasi-uniform distribution. At the scale of whole metasurface dimensions, the field distribution is close to sinusoidal in both x and y directions.

The metasurface has been fabricated whose geometry is in accordance with the simulation. The proof-of-concept experiments have been performed. The schematic of the experimental setup and photo of the metasurface are presented in Fig 7 (a) and (b), respectively.

The experimental setup is depicted in Fig.7 (a). The first port of VNA was used to excite the metasurface via an SMA connector mounted in the gap of the lateral wire. The receiving port of VNA was connected to a receiving (Rx) loop whose position was controlled by the 3D scanner. To measure the efficiency over the metasurface, the scanning plane was z = 15 mm above the top wire layer of the metasurface, assuming that the top wire layer is in the plane z = 0 mm. At each Rx position the complex value of the transmission coefficient was recorded and used in post-processing to calculate the magnetic field distribution and WPT efficiency.

III. MAGNETIC FIELD DISTRIBUTION

The measured input admittance is compared to the simulated one in Fig. 6 (a). The resonant frequency determined at the maxima is 19.6 MHz. A slight deviation of the measured resonant frequency with respect to the simulated one can be explained by the fabrication tolerances and water permittivity deviation. The Q-factor extracted from the measured data is 270. Compared to the simulated Q-factor, its degradation was due to the higher dielectric losses of the real water host than one considered in the simulation. A quasi-uniform field distribution in the central area can be seen in Fig. 6 (c), which corresponds to the numerically simulated one in Fig. 6 (b).

IV. WPT EFFICIENCY

WPT efficiency has been numerically and experimentally studied. A rectangular loop with the size of 9 cm × 6 cm was used as a receiver. It was made of a copper wire with the radius of 1 mm. The WPT efficiency was determined through the S-parameters as $\eta = |S_{21}|^2$, when the reflection coefficients at both the Rx and Tx ports of the system are equal to zero ($S_{11} = 0$, $S_{22} = 0$), which corresponds to the maximum achievable power transfer of a two–port network [34], [35]. Thus, additional conjugate matching networks were used to satisfy this condition.

The numerical simulations of the WPT efficiency of the system were performed in CST Microwave Studio. The Rx loop was placed in the plane z = 15 mm above the metasurface and was moved with a step of 10 mm over the entire metasurface area to estimate the uniformity of the transmitted power. In Fig. 7 (c), the WPT efficiency of more than 80% was obtained over the central area of the metasurface. The WPT efficiency extracted from the measured data is shown in Fig. 7 (d). WPT efficiency higher than 70% was obtained. Compared to the simulated WPT efficiency, the measured one was less due to the dissipation losses in the water. Nevertheless, it was both numerically and experimentally proved that

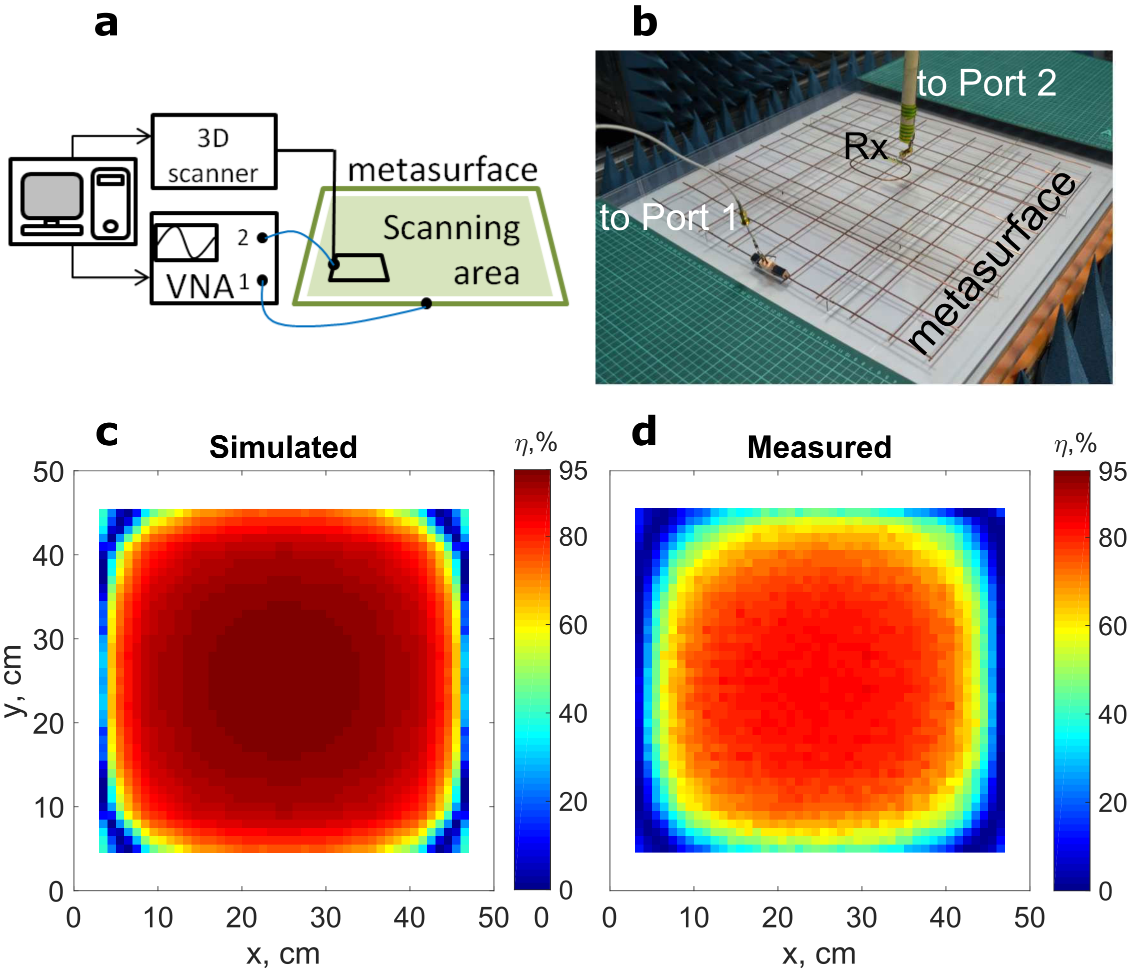

FIGURE 7. **(a) Experimental setup and (b) photograph of the metasurface prototype. (c) Simulated and (d) measured WPT efficiency.**

the proposed metasurface provides efficient (at least 70%) free-positioning power transmission over 40 × 40 cm^2 area which is comparable to an office desktop area.

V. ELECTRIC FIELD AND SAR ASSESSMENT

Despite the fact that the magnetic field is needed for the power transfer, the electric field is undesired above the plane of the transmitter due to safety reasons [20], [21]. Thus, it is highly important to confine it as much as possible in the interior of the Tx resonator. To demonstrate that the proposed metasurface resonator has a peculiar property to separate electric and magnetic near-field, we compared metasurface resonator with a conventional planar coil resonator. The comparison was based on the following two assumptions. First, we assume that both systems have the same WPT performance, or, in other words, when the Rx is placed at the same position with respect to the Tx, the WPT efficiency is the same. Second, we consider both transmitters have the same charging area, i.e. the magnetic fields have similar intensity and distribution. Therefore, the planar coil resonator was designed under this criterion. It was made from a five-turn spiral with wire radius of 1 mm and wire spacing 5.56 cm. To tune the resonant frequency of the spiral coil to 19.2 MHz, a 2.6 pF capacitor was connected in series to the port. The simulated magnetic field was distributed quasi-uniformly in the central area of coil, which is similar to that of the metasurface, thereby resulting in a same WPT efficiency of 92.4 %.

The magnetic field distribution of the metasurface remains similar to that of spiral coil. Fig. 8(g) shows the z-component of the magnetic field on the diagonal cross section and Fig. 8(h) shows magnetic field decays along the white dashed line in Fig. 8(g). However, a considerable difference was found in the electric field distributions created by the two structures, see Fig. 8 (c) and (d). Compared to the planar resonator, the electric field above the metasurface is greatly reduced. The electric field reduction originates from the redistributed electric and magnetic fields provided by the unique metasurface structure. Here, the structure provided distributed capacitance which existed in the corner areas of the metasurface between two layers of wires, as shown in Fig. 8 (c). Fig. 8 (e) and (f) further show the electric field distributions of both metasurface and the spiral coil

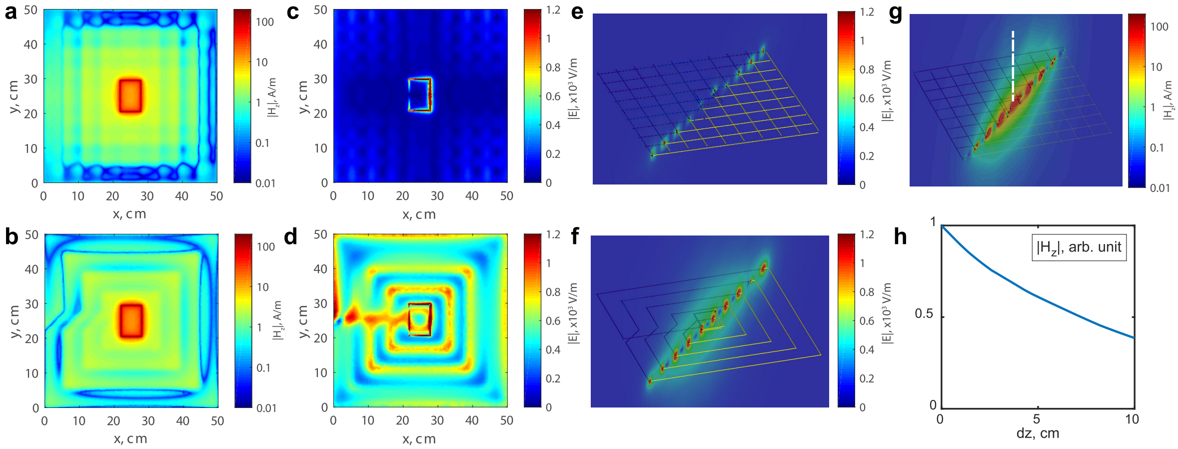

FIGURE 8. Simulated z-component of magnetic field distribution on the plane z = 15 mm for (a) metasurface and (b) spiral coil, and (g) on the diagonal cross section for metasurface, and (h) field decay along white dashed line in the subplot (g). Electric field distribution on the plane z = 15 mm for (c) metasurface and (d) spiral coil. Electric field distribution on the diagonal cross section for (e) metasurface and (f) spiral coil.

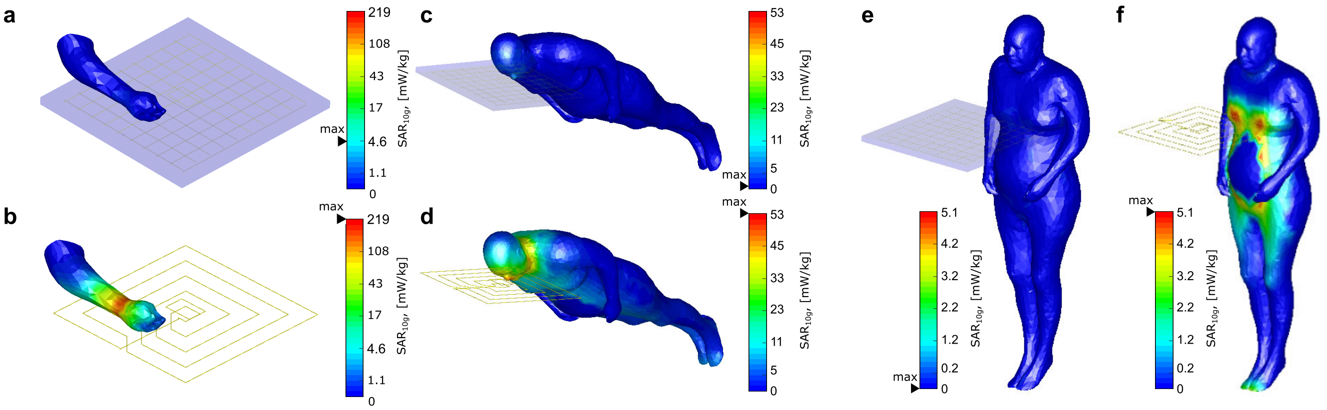

FIGURE 9. Comparison of the simulated SAR 10g patterns of (a,c,e) the metasurface and (b,d,f) the spiral coil in the presence of forearm and human body models under 1 W input power.

TABLE 1. Comparison of WPT efficiency and SAR under 1 W input power.

	Tx type	human-free	forearm	stand	head
WPT efficiency, %	Metasurface	92.4	92.1	92.1	91.7
	Spiral coil	92.4	86.1	91.0	84.4
SAR, mW/kg	Metasurface	-	4.6	0.01	1.6
	Spiral coil	-	219	5.1	53

on the diagonal cross section. Compared to the planar resonator, the electric field in the metasurface is mostly confined between two wire layers and it barely leaks to the upper space.

The SAR analysis was numerically performed in CST Microwave Studio. A computer-aided design (CAD) model of a human forearm and full body (Female VHP CAD model) were used to demonstrate three different scenarios: human forearm put on the top of the transmitter at z = 15 mm, see Fig. 9 (a,b); human head facing down to the transmitter at z = 20 mm, see Fig. 9 (c,d); and human standing 25 mm away from the transmitter, see Fig. 9 (e,f). The human body model contained the detailed biological tissues (skin, fat, muscle, bone, blood, etc) that were characterized by their corresponding electromagnetic properties.The simulations have been done for 1 W of input power for both systems.

The WPT efficiencies and peak average SAR_{10g} are summarized in Table 1. In the absence of human model, the maximal WPT efficiencies for both metasurface and spiral coil systems were 92.4 %. However, the human body interacts with spiral coil system much more significantly than with metasurface. It's worth noting that the presence of the human head deteriorated the WPT efficiency as much as by 8 % for the spiral coil system, whereas the efficiency dropped only 0.7 % for the metasurface based system. A greater portion of electric energy is dissipated inside the human body due to the stronger interaction between human tissue and WPT system. On the contrary, the human body barely interacts with the metasurface and thereby it does not influence the input impedance of metasurface transmitter, as shown by the blue solid line in Fig. 6(a). The power dissipation in the human body results in heat generation which can be evaluated by SAR. For the human forearm case, the peak SAR_{10g} of the metasurface based system is 4.6 mW/kg which is 47 times lower than the planar resonator based system. Therefore, under the IEEE safety regulation [36], which is 4W/kg for the limbs and 2W/kg for head and trunk, the maximum power of 869 W for the metasurface is allowed, whereas only 18 W is permitted for the spiral coil system.

VI. CONCLUSION

To sum up, we have proposed the metasurface transmitter, numerically and experimentally studied the metasurface. The quasi-uniform magnetic field distribution over the area of 40×40 cm^2 is demonstrated numerically and experimentally verified by near-field measurements, which has potential practical values for charging multiple receivers. The essential advantage of the proposed metasurface is that electric and magnetic near fields are well separated at the operational frequency, where the former is confined inside the structure. Here, it has been numerically and experimentally proved that the proposed metasurface provides efficient (at least 70 %) free-positioning power transmission over 40×40 cm^2 area which is comparable to an office desktop size. Compared to the planar spiral-coil based system, a 47 times reduction of peak SAR value in the metasurface-based system has been achieved. The proposed design paves a way to a new generation of WPT transmitters for high-power charging scenarios with much reduced electric field leakage.

ACKNOWLEDGMENT

(Aleksandr Markvart and Mingzhao Song contributed equally to this work.) The authors appreciate the useful discussions with G. Solomakha and R. Balafendiev.

REFERENCES

[1] S. D. Barman, A. W. Reza, N. Kumar, M. E. Karim, and A. B. Munir, "Wireless powering by magnetic resonant coupling: Recent trends in wireless power transfer system and its applications," *Renew. Sustain. Energy Rev.*, vol. 51, pp. 1525–1552, Nov. 2015.

[2] M. Song, P. Belov, and P. Kapitanova, "Wireless power transfer inspired by the modern trends in electromagnetics," *Appl. Phys. Rev.*, vol. 4, no. 2, Jun. 2017, Art. no. 021102.

[3] M. Abou Houran, X. Yang, and W. Chen, "Magnetically coupled resonance WPT: Review of compensation topologies, resonator structures with misalignment, and EMI diagnostics," *Electronics*, vol. 7, no. 11, p. 296, Nov. 2018.

[4] Z. Zhang, H. Pang, A. Georgiadis, and C. Cecati, "Wireless power transfer—An overview," *IEEE Trans. Ind. Electron.*, vol. 66, no. 2, pp. 1044–1058, Feb. 2019.

[5] A. Kurs, A. Karalis, R. Moffatt, J. D. Joannopoulos, P. Fisher, and M. Soljacic, "Wireless power transfer via strongly coupled magnetic resonances," *Science*, vol. 317, no. 5834, pp. 83–86, Jul. 2007.

[6] A. Karalis, J. D. Joannopoulos, and M. Soljačić, "Efficient wireless non-radiative mid-range energy transfer," *Ann. Phys.*, vol. 323, no. 1, pp. 34–48, Jan. 2008.

[7] B. Wang, W. Yerazunis, and K. H. Teo, "Wireless power transfer: Metamaterials and array of coupled resonators," *Proc. IEEE*, vol. 101, no. 6, pp. 1359–1368, Jun. 2013.

[8] S. Yu, H. Liu, and L. Li, "Design of near-field focused metasurface for high-efficient wireless power transfer with multifocus characteristics," *IEEE Trans. Ind. Electron.*, vol. 66, no. 5, pp. 3993–4002, May 2019.

[9] A. L. A. K. Ranaweera, T. S. Pham, H. N. Bui, V. Ngo, and J.-W. Lee, "An active metasurface for field-localizing wireless power transfer using dynamically reconfigurable cavities," *Sci. Rep.*, vol. 9, no. 1, pp. 1–12, Aug. 2019.

[10] M. Song, K. Baryshnikova, A. Markvart, P. Belov, E. Nenasheva, C. Simovski, and P. Kapitanova, "Smart table based on a metasurface for wireless power transfer," *Phys. Rev. Appl.*, vol. 11, no. 5, May 2019, Art. no. 054046.

[11] S. Assawaworrarit, X. Yu, and S. Fan, "Robust wireless power transfer using a nonlinear parity–time-symmetric circuit," *Nature*, vol. 546, pp. 387–390, Jun. 2017.

[12] Y. Ra'Di, B. Chowkwale, C. Valagiannopoulos, F. Liu, A. Alù, C. R. Simovski, and S. A. Tretyakov, "On-site wireless power generation," *IEEE Trans. Antennas Propag.*, vol. 66, no. 8, pp. 4260–4268, Aug. 2018.

[13] S. Wang, Z. Hu, C. Rong, C. Lu, J. Chen, and M. Liu, "Planar multiple-antiparallel square transmitter for position-insensitive wireless power transfer," *IEEE Antennas Wireless Propag. Lett.*, vol. 17, no. 2, pp. 188–192, Feb. 2018.

[14] J. J. Casanova, Z. Ning Low, J. Lin, and R. Tseng, "Transmitting coil achieving uniform magnetic field distribution for planar wireless power transfer system," in *Proc. IEEE Radio Wireless Symp.*, Jan. 2009, pp. 530–533.

[15] J. J. Casanova, Z. Ning Low, and J. Lin, "A loosely coupled planar wireless power system for multiple receivers," *IEEE Trans. Ind. Electron.*, vol. 56, no. 8, pp. 3060–3068, Aug. 2009.

[16] L. Shen, W. Tang, H. Xiang, and W. Zhuang, "Uniform magnetic field of the planar coil with new winding structure for displacement-insensitive WPT," in *Proc. IEEE Int. Conf. Commun. Problem-solving*, Dec. 2014, pp. 394–396.

[17] X. Liu and S. Y. Hui, "Optimal design of a hybrid winding structure for planar contactless battery charging platform," *IEEE Trans. Power Electron.*, vol. 23, no. 1, pp. 455–463, Jan. 2008.

[18] D. Yinliang, S. Yuanmao, and G. Yougang, "Design of coil structure achieving uniform magnetic field distribution for wireless charging platform," in *Proc. 4th Int. Conf. Power Electron. Syst. Appl.*, Jun. 2011, pp. 1–5.

[19] E. Waffenschmidt, "Free positioning for inductive wireless power system," in *Proc. IEEE Energy Convers. Congr. Expo.*, Sep. 2011, pp. 3480–3487.

[20] C. Mohamed, V. Guillaume, and T. Alexandru, "Compliance assessment of human body exposure to wireless power systems," in *Proc. 2nd World Congr. Electr. Eng. Comput. Syst. Sci.*, Jul. 2016, pp. 448–451.

[21] P. Rasic, M. Skiljo, Z. Blazevic, V. Doric, and D. Poljak, "Simulation of human body exposure to high and low frequency wireless power transfer systems using simplified models," in *Proc. 3rd Int. Conf. Smart Sustain. Technol. (SpliTech)*, Jun. 2018, pp. 1–6.

[22] J. Chakarothai, W. Kanako, and S. Watanabe, "Evaluation of EM absorption characteristics in realistic adult and child models in vicinity of wireless power transfer systems," in *Proc. Asia–Pacific Symp. Electromagn. Compat. (APEMC)*, May 2015, pp. 448–451.

[23] T. Shimamoto, M. Iwahashi, Y. Sugiyama, I. Laakso, A. Hirata, and T. Onishi, "SAR evaluation in models of an adult and a child for magnetic field from wireless power transfer systems at 6.78 MHz," *Biomed. Phys. Eng. Express*, vol. 2, no. 2, Mar. 2016, Art. no. 027001.

[24] J. Nadakuduti, M. Douglas, L. Lu, A. Christ, P. Guckian, and N. Kuster, "Compliance testing methodology for wireless power transfer systems," *IEEE Trans. Power Electron.*, vol. 30, no. 11, pp. 6264–6273, Nov. 2015.

[25] A. Christ, M. G. Douglas, J. M. Roman, E. B. Cooper, A. P. Sample, B. H. Waters, J. R. Smith, and N. Kuster, "Evaluation of wireless resonant power transfer systems with human electromagnetic exposure limits," *IEEE Trans. Electromagn. Compat.*, vol. 55, no. 2, pp. 265–274, Apr. 2013.

[26] F. Lemoult, G. Lerosey, J. de Rosny, and M. Fink, "Resonant metalenses for breaking the diffraction barrier," *Phys. Rev. Lett.*, vol. 104, no. 20, May 2010, Art. no. 203901.

[27] A. P. Slobozhanyuk, A. N. Poddubny, A. E. Krasnok, and P. A. Belov, "Magnetic purcell factor in wire metamaterials," *Appl. Phys. Lett.*, vol. 104, no. 16, Apr. 2014, Art. no. 161105.

[28] A. P. Slobozhanyuk, A. N. Poddubny, A. J. Raaijmakers, C. A. van Den Berg, A. V. Kozachenko, I. A. Dubrovina, I. V. Melchakova, Y. S. Kivshar, and P. A. Belov, "Enhancement of magnetic resonance imaging with metasurfaces," *Adv. Mater.*, vol. 28, no. 9, pp. 1832–1838, 2016.

[29] A. D. Yaghjian and S. R. Best, "Impedance, bandwidth, and Q of antennas," *IEEE Trans. Antennas Propag.*, vol. 53, no. 4, pp. 1298–1324, Apr. 2005.

[30] W. Ellison, "Permittivity of pure water, at standard atmospheric pressure, over the frequency range 0–25 THz and the temperature range 0–100°C," *J. Phys. Chem. Reference Data*, vol. 36, no. 1, pp. 1–18, 2007.

[31] V. Komarov, S. Wang, and J. Tang, "Permittivity and measurements," in *Encyclopedia of RF and Microwave Engineering*. 2005. [Online]. Available: https://onlinelibrary.wiley.com/doi/abs/10.1002/0471654507.eme308, doi: 10.1002/0471654507.eme308.

[32] A. Klein and N. Katz, "Strong coupling optimization with planar spiral resonators," *Current Appl. Phys.*, vol. 11, no. 5, pp. 1188–1191, Sep. 2011.

[33] F. Jolani, Y. Yu, and Z. Chen, "A planar magnetically coupled resonant wireless power transfer system using printed spiral coils," *IEEE Antennas Wireless Propag. Lett.*, vol. 13, pp. 1648–1651, 2014.

[34] S. Roberts, "Conjugate-image impedances," *Proc. IRE*, vol. 34, no. 4, pp. 198p–204p, Apr. 1946.

[35] Q. Wang, W. Che, G. Monti, M. Mongiardo, M. Dionigi, and F. Mastri, "Conjugate image impedance matching for maximizing the gains of a WPT link," in *IEEE MTT-S Int. Microw. Symp. Dig.*, May 2018, pp. 1–3.

[36] *IEEE standard for safety levels with respect to human exposure to radio frequency electromagnetic fields, 3 khz to 300 GHz*, IEEE Standard C95.1-2005, IEEE Standards Department, International Committee on Electromagnetic Safety, The Institute of Electrical and Electronics Engineers, New York, NY, USA, 2005.

ALEKSANDR MARKVART received the B.Sc. and M.Sc. degrees in radiophysics from Peter the Great St. Petersburg Polytechnic University (SPbPU), Russia, in 2015 and 2017, respectively, where he is currently pursuing the Ph.D. degree. His current research interests include wireless power transfer, microwave devices, and fiber optics.

MINGZHAO SONG received the bachelor's degree in information science and electrical engineering from Zhejiang University, China, in 2012, and the master's degree in photonics and optoinformatics and the Ph.D. degree in nanophotonics and metamaterials from ITMO University, Russia, in 2015 and 2019, respectively. His current research interests include wireless power transfer and metamaterials.

STANISLAV GLYBOVSKI was born in Syktyvkar, Russia, in 1987. He received the M.Sc. and Ph.D. degrees in radiophysics from St. Petersburg State Polytechnic University, St. Petersburg, Russia, in 2010 and 2013, respectively. He is currently an Associate Professor with the Department of Nanophotonics and Metamaterials, ITMO University, St. Petersburg. His current research interests include antennas and microwave devices, computational electromagnetics, metamaterials, and MRI.

PAVEL BELOV was born in U.S.S.R., in 1977. He received the degree (Hons.) from ITMO University, St. Petersburg, in 2000. He defended his Ph.D. thesis twice: once in Russia, in 2003, and then in Finland, in 2006, at the Helsinki University of Technology, Espoo, Finland. He is currently the Dean of the Physics and Engineering Faculty and the Head of the Research Center of Nanophotonics and Metamaterials, ITMO University. His current research interests include metamaterials, plasmonics, electromagnetics, nanophotonics, antennas, and nanostructures.

CONSTANTIN SIMOVSKI defended his Ph.D. thesis at Russian University, currently called as St. Petersburg Polytechnical University, in 1986. In 2000, he defended the D.Sc. thesis in physics and mathematics at St. Petersburg Polytechnical University. He has worked in both industry and academia. Since 2008, he has been with the Helsinki University of Technology, currently Aalto University. His current researches focus on new metamaterials for nanosensing, energy harvesting, nanophotonic components, and the electromagnetic characterization of metamaterials.

POLINA KAPITANOVA was born in Saint-Petersburg, Russia. She received the bachelor's, master's, and Ph.D. degrees in electrical engineering and telecommunications from Saint Petersburg Electrotechnical University, Russia, in 2004, 2006, and 2011, respectively. She is currently an Associate Professor at ITMO University, Russia. Her scientific interests include design and development of metamaterials and metasurfaces, wireless power transfer technologies, and antenna engineering.